

**TJPS****The Thai Journal of Pharmaceutical Sciences**
39 (4), October - December 2015: 141-148

Cocrystallization of Artemisinin and Amodiaquine Hydrochloride

Wiriyaporn Sirikun¹, Jittima Chatchawalsaisin^{1,2}, Narueporn Sutanthavibul^{1,2*}¹Faculty of Pharmaceutical Sciences, Chulalongkorn University, Bangkok, 10330 Thailand²Chulalongkorn University Drug and Health Products Innovation Promotion Center (CU.D.HIP), Faculty of Pharmaceutical Sciences, Chulalongkorn University, Bangkok, 10330 Thailand

Abstract

Artemisinin (ART) and amodiaquine dihydrochloride dihydrate (AQD) was selected as model host and guest molecules in the study. Cocrystallization of ART and AQD at mole ratio of 1:1 by temperature change technique using ethanol resulted in new solid state structure (Rec-ART-AQD (1:1)). The cocrystallized structure exhibited different XRPD pattern from ART, AQD and amodiaquine dihydrochloride monohydrate (AQM). In addition, FT-IR spectrogram of Rec-ART-AQD (1:1) showed shift in wavenumber from 3440 cm⁻¹ to a lower region. This shift was due to the hydrogenbonding of -NH functional group on AQM interacting with C=O of ART. Thermal analysis of Rec-ART-AQD (1:1) also showed lower average endothermic dehydration energy and started at slightly lower temperature than AQM which was in good agreement with TGA results. Rec-ART-AQD (1:1) was analyzed for each component by HPLC. Analytical result showed that Rec-ART-AQD (1:1) contained 3.50% w/w of ART signifying ART: AQM mole ratio of 1:16 in the cocrystals. Solubility of ART in Rec-ART-AQD (1:1) at 30 °C is 79.87 µg/mL which was 33.41 % higher than ART solubility (59.87 µg/mL). Rec-ART-AQD (1:1) was found to have good stability with negligible water vapor uptake under various humidity generated by dynamic vapor sorption (DVS) study. Rec-ART-AQD (1:1) showed slight increase in antimalarial activity against *P. falciparum* compare to AQD and AQM. From the above supporting results, crystals obtained by recrystallization of ART together with AQD were cocrystals with uniform distribution of individual ART molecules in the major crystalline lattice of AQM at a mole ratio of 1:16.

Keywords: Cocrystallization, artemisinin, amodiaquine dihydrochloride monohydrate, solid state characterization, physicochemical characterization

Correspondence to: Narueporn Sutanthavibul, Ph.D.
Chulalongkorn University Drug and Health Products Innovation
Promotion Center (CU.D.HIP), Faculty of Pharmaceutical
Sciences, Chulalongkorn University
254 Phyathai Road, Pathumwan, Bangkok, 10330 Thailand
E-mail: narueporn.s@chula.ac.th

Received: 12 June 2015

Revised: 4 August 2015

Accepted: 14 August 2015

Academic Editor: Wanchai De-Eknamkul

Introduction

Cocrystals are newly defined solid morphology which becomes increasingly promising for drug development especially improving drug solubility and high potential on intellectual property rights [1-4]. Cocrystals are defined as the formation of a crystalline state between molecular or ionic active pharmaceutical ingredients (API) and cocrystal former that is normally solid under ambient condition [5]. Cocrystals are dramatically different from salts [6-8]. Cocrystals are formed via H-bond formation, while salts are formed by ionic interaction [9]. Particularly useful are carboxylic acid functional groups which commonly form H-bonds with other molecules to produce cocrystals. Other functional groups which are of interested are amine and

amide groups. Nevertheless, other functional groups have also been studied such as cocrystal between alcohol and amine or cocrystal between alcohol and pyridine [5]. The crystallization techniques commonly used to generate cocrystals are slow evaporation, sublimation, growth from melt, slurries, grinding and solvent drop grinding [5].

Artemisinin (*ginghaosu*) was found to be an efficacious drug to date against multidrug-resistance *Plasmodium falciparum* malaria [10-13]. Artemisinin is a sesquiterpene lactone with antimalarial activity due to endoperoxide trioxane moiety [10]. Artemisinin is a highly crystalline compound that will not dissolve in water or oil [12]. The formulation difficulties and bioavailability problems of artemisinin are mainly due to this lack of solubility [12]. Therefore, the World Health Organization (WHO) requested the drug companies to stop manufacturing “single drug” artemisinin despite that it is the most efficacious drug to date. They have found that artemisinin only weakens the parasite but not totally kills it, hence, inducing recrudescence (due to its short half-life) and ultimately drug resistance. Currently, WHO suggested an “Artemisinin Combination Therapies” (ACTs) as ideal therapy [10, 14].

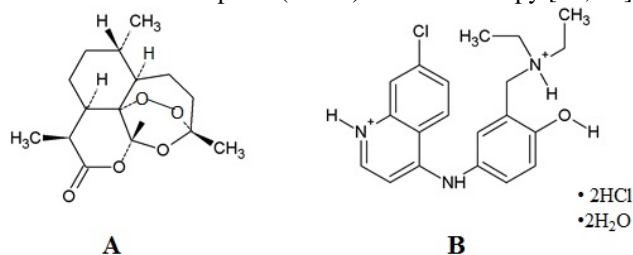


Figure 1 (A) The structure of artemisinin and (B) the structure of amodiaquine dihydrochloride dihydrate.

Numbers of researchers have studied cocrystal formation between two small molecules or a molecular or ionic active pharmaceutical ingredient (API) and other smaller cocrystal formers with dominant hydrogen-bonding interactions [16]. Examples of cocrystals produced by other researchers are theophylline-caffeine [7], carbamazepine-nicotinamide [5] and celecoxib-nicotinamide [15]. In this study, artemisinin (ART) was selected for cocrystallization screening in order to improve its solubility. The selected complementary drug, amodiaquine dihydrochloride dihydrate (AQD), has higher solubility than ART and the selection was based on drug species normally used in ACTs [17-18]. This study is the first study which both entities are large molecules and APIs. Both are able to form hydrogen-bonds, through carbonyl group (C=O) (known as hydrogen bond acceptor) of ART (Figure 1 (A)) and amine (-NH₃) and hydroxyl (-OH) groups (H bond donor) of AQD (Figure 1 (B)). The objective of this study is to evaluate the cocrystal formation between ART and AQD in the same cocrystallizing condition with the aim of improving ART solubility.

Materials and Methods

Materials

The starting materials in this study were artemisinin (ART) obtained from Honghao Chemicals (Shanghai, China) and amodiaquine dihydrochloride dihydrate (AQD) purchased from Sigma Aldrich (St. Louis, MO). Anhydrous ethanol obtained from Carlo Erba, Val de Reuil, France, was used as a solvent for polymorphic screening.

Methods

Cocrystallization

Cocrystallization of ART and AQD were carried out using ethanol by temperature change technique. In ethanol environment, mole ratios of ART to AQD were varied as 1:1, 1:1.25, 1:1.5, and 1:2. The solid ART and AQD mixtures were introduced into 25 mL of ethanol. Initially each mixture showed turbid solution at 30 °C, when heated to 50 °C for 10 minutes, clear solutions were observed. The solutions were then cool-down in a circulating water bath (Polystat Control cc1, Huber, Germany) with a controlled temperature of 30 °C for 2 days until small crystal nuclei appeared. The samples were then kept at 30 °C to allow crystal nucleation to mature. The fully grown crystals were then harvested and washed by ethanol. Crystals were then allowed to dry at room temperature. ART and AQD were recrystallized separately according to the method above. The crystal mixtures were then separated under polarized light microscope to select appropriate newly formed crystal habits. Criteria for crystal selection were that the recrystallized crystals should not aggregate but must be opaque. The selected crystals were further undergone solid state characterization, chemical analysis and physicochemical evaluation.

Solid state characterization

The recrystallized crystals obtained were subjected to the following characterization procedures;

Polarized light microscopy

Crystals were observed under polarized light microscope (Eclipse E200, Nikon, Japan) to select the desired crystals from various crystal habits obtained by recrystallization and cocrystallization. The appropriate crystals were identified visually under polarized light microscope which will be used throughout this article.

X-ray powder diffractometry (XRPD)

Each recrystallized and cocrystallized crystals were identified by X-ray powder diffractometry (XRPD) on Miniflex II (Rigaku, Japan). Wide angle XRPD using CuK α radiation at 40 kV and 20 mA was employed. The scan speed was held constant at 1° per min and the angular scanning range was programmed from 5 to 40° 2 θ .

Differential scanning calorimetry (DSC)

Thermal behaviors of the samples were evaluated by DSC using DSC 822^o (Mettler Toledo, Switzerland). Accurately weighed approximately 3 mg of the sample and placed in a 40 μ L standard aluminium pan. The pan was hermetically sealed and punctured with one pin hole. The scanning rate was held constant at 10 $^{\circ}$ C/min and the scanning temperature range was from 25 $^{\circ}$ C to 250 $^{\circ}$ C. Dried nitrogen gas at the rate of 60 mL/min was purged throughout the study to avoid oxidative decomposition upon heat treatment. DSC calibration using standard indium was periodically done. Evaluation of the diffractograms obtained by DSC was done using STAR^o software for data processing.

Crystals which were found to have possibility of forming new solid state structure(s) will be further characterized by the following studies.

Fourier transform infrared spectroscopy (FT-IR)

The samples were thoroughly mixed with dried KBr powder and finely ground in an agate mortar. The sample-KBr mixtures were then transferred between two stainless steel punches and compressed with a hydraulic press to form compact pellets. Infrared spectra were obtained by an infrared light source at 20 scans and 4.00 cm^{-1} resolution. The spectral wave number was collected from 4000-400 cm^{-1} by Spectrum One Fourier transform infrared spectrometer (Perkin Elmer, USA).

Thermogravimetric Analysis (TGA)

Accurately weighed approximately 2 mg of sample and placed in a 70 μ L alumina sample holder. TGA (TGA/SDTA851^o, Mettler Toledo, Switzerland) was done using scanning rate of 10 $^{\circ}$ C/min and the temperature range was from 25 $^{\circ}$ C to 250 $^{\circ}$ C. Dried nitrogen gas at the rate of 60 mL/min was purged throughout the study to avoid oxidative decomposition upon heat treatment. Evaluation for the TGA weight loss behavior was done by using STAR^o software for data processing.

Scanning Electron Microscopy (SEM)

Crystal habits were observed in detail by scanning electron microscopy (SEM). Samples were carefully placed on the metal stub where it was then sputter-coated with gold under vacuum before the morphology was recorded by SEM (JSM-5410LV, JEOL, Japan).

Chemical analysis

Chemical analysis was done to evaluate the ratio of ART to AQD in the suspected cocrystals produced.

High Performance Liquid Chromatography (HPLC)

Sample preparation

To evaluate the amount of ART in recrystallized crystals, one milligram of the selected crystals obtained from cocrystallization was dissolved in 2 mL of acetonitrile in water (1:1). The final concentration of 0.5 mg/mL was filtered through 0.45 μ m nylon (VertiPureTM) membrane filter.

Condition

HPLC analysis of ART was modified from the artemisinin monograph in the International Pharmacopeia 2003. The present method used gradient condition (Table 1) with diode-array detector. Mobile phase consisted of water: acetonitrile (2:3). The sample was pumped through Inertsil^o ODS-3 4.6x250 mm (with 5 μ m particle sizes as stationary phase) at a flow rate of 1.0 mL/min. The sample was evaluated at a wavelength of 201 nm.

Table 1 HPLC gradient condition for the analysis of ART.

Time (min)	Water (%v/v)	Acetonitrile (%v/v)
0-17	40	60
17-18	40 to 0	60 to 100
18-19	0	100
19-20	0 to 20	100 to 80
20-28	20	80
28-29	20 to 40	80 to 60
29-65	40	60

Physicochemical analysis

To study the effect of water on the proposed cocrystal structure(s), all samples were evaluated for their responses after exposure to water in the liquid or vapor states.

Dynamic vapor sorption (DVS)

Transformation of recrystallized crystals due to water vapor was monitored by dynamic vapor sorption (DVS) apparatus (Intrinsic, Surface Measurement Systems, Ltd, UK). Adsorption isotherms were obtained at a controlled temperature of 30 $^{\circ}$ C. The samples were exposed to increment at increase in relative humidity (RH) from 0 % RH to 100 % RH. Changes in the sample weight were periodically recorded.

Solubility profiles of ART

Excess ART crystals were placed in 14 mL vessels containing purified water immersed in circulating water bath at a controlled temperature of 30 $^{\circ}$ C. The amounts of dissolved ART were evaluated at 15, 60 and 180 minutes. The sample collected at each time period was filtered through 0.45 μ m nylon (VertiPureTM) membrane filter, diluted with appropriate solvents and evaluated by HPLC method mentioned previously.

For recrystallized crystals, the experiment can not be done with excess amounts due to limited number of crystals

obtained per batch. Alternatively, the solubility of the crystal was evaluated by accurately weighing predetermined recrystallized crystals and placed in vessels containing purified water immersed in circulating water bath at a controlled temperature of 30 °C. The amounts of dissolved ART were evaluated at 15, 60 and 180 minutes. Sample collected at each time period was filtered by 0.45 µm nylon (VertiPure™) membrane filter, diluted with appropriate solvents and analyzed by HPLC.

In-vitro antimalarial test (Microculture radioisotope technique)

The *in-vitro* antimalarial tests of recrystallized crystals, control group and starting material of ART and AQD were evaluated. Samples were dissolved in dimethyl sulfoxide (DMSO) and the final concentration of samples was adjusted to 10 mg/mL. The diluted samples were tested against *Plasmodium falciparum*; K1 Strain. Inhibition concentrations (IC₅₀) were recorded for the positive controls which were dihydroartemisinin (1.35 nM) and mefloquine (0.0268 µM), and the negative control was 0.1 % DMSO. (Remark: The test was done at National Center for Genetic Engineering and Biotechnology: BIOTEC, Thailand Science Park, Pathum Thani, Thailand)

Results and Discussion

Cocrystallization of ART and AQ

From the XRPD results, cocrystallization of ART and AQD at 1:1 mole ratio showed optimum starting amounts of reactants (ART and AQD) (data not shown). An increased amount of ART or AQD in both directions, resulted in the dominant characteristics of the reactants whichever are present in greater amount. When ART and AQD were separately recrystallized under the same cocrystallization condition, ART did not change but AQD converted to amodiaquine dihydrochloride monohydrate (AQM) form. XRPD results of ART and AQD cocrystallized at 1:1 mole ratio showed XRPD patterns similar to AQM but with the appearance of additional peak positions at 13.4, 16.2, 23.8, and 29.8°2θ, and with absent peak at 28.2°2θ (Figure 2). From the results, the cocrystallized crystals of ART and AQD at 1:1 mole ratio in ethanol was selected for further evaluations and will be presented as Rec-ART-AQD (1:1).

To identify the differences in Rec-ART-AQD (1:1) to AQM, samples were further evaluated by FT-IR and compare to the starting materials (ART and AQD). ART spectrum showed dominant peak at 1738 cm⁻¹ representing C=O functional group (Figure 3). While FT-IR spectra of Rec-ART-AQD (1:1) and AQM in Figure 3 were similar but dramatically different from ART and AQD. However, there are some notable differences on FT-IR spectra between AQM and Rec-ART-AQD (1:1) despite their similarities. The peak at 3440 cm⁻¹ was absent in Rec-ART-AQD (1:1)

where it represents non hydrogen bonded –NH stretching on both AQM and AQD. The absence of 3440 cm⁻¹ in Rec-ART-AQD (1:1) may be due to H-bonded interaction with ART at that –NH functional group, hence, diminishing its peak.

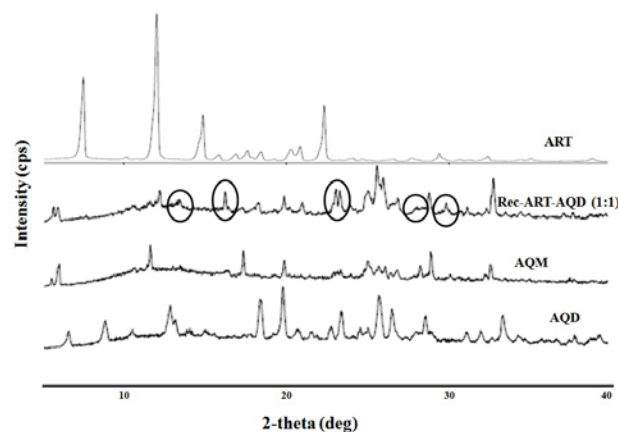


Figure 2 XRPD Diffractograms of crystals obtained by cocrystallization of ART and AQD by temperature-change technique using ethanol as solvent compare to the starting materials.

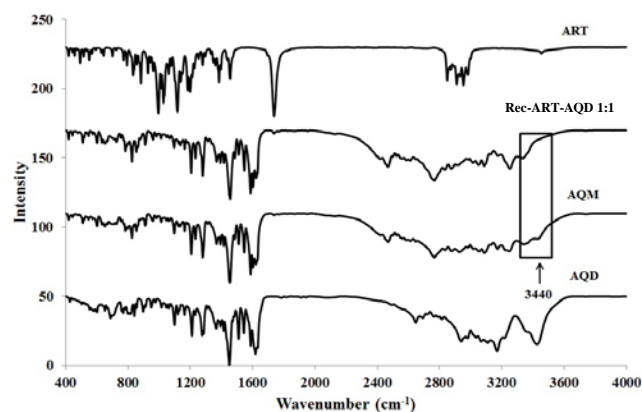


Figure 3 FT-IR spectra of starting materials (ART and AQD) and recrystallized crystals; AQM and Rec-ART-AQD (1:1).

As a result from FT-IR study, the possible H-bonding sites for ART and AQM are postulated in Figure 4. The first evidence for H-bonding was seen as the wavenumber at 3440 cm⁻¹ for secondary amine stretching (-NH stretching) was absent at N2 position of AQD in Rec-ART-AQD (1:1). This may be due to the peak shift to lower wave number when electrons of hydrogen in secondary amine were withdrawn towards a higher electronegativity oxygen atom in C=O functional group of ART. The second possible H-bonding site may be between C19 of AQD and O4 of ART where they shared the electrons of H from C19 position in AQM. However, no evidence from FT-IR was shown, due to the

possibility of the very low signal and the overlapping nature of C19 in aromatic group in AQD. FT-IR signals obtained from ART functional group in Rec-ART-AQD (1:1) spectrum were all very low and could not be separately identified in Rec-ART-AQD (1:1).

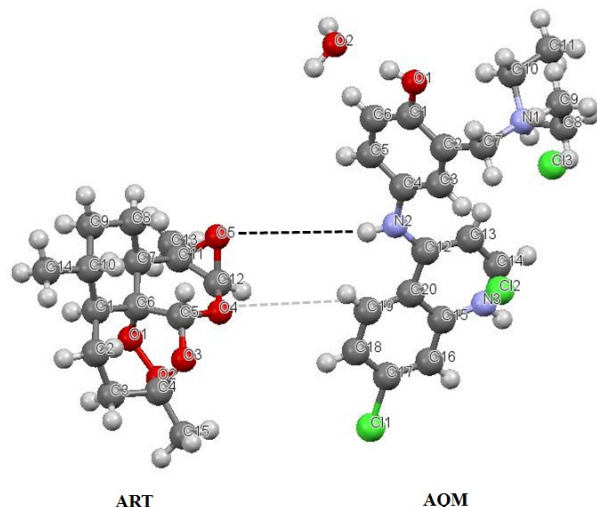


Figure 4 The postulated H-bonding sites for ART and AQM from evidence obtained by FT-IR studies.

Table 2 The comparison of endothermic energy calculated for AQM and Rec-ART-AQD (1:1) from DSC thermograms at a heating rate of 10 °C/minute from 25-250 °C.

Sample	Energy (J/g)		
	(170 °C)	(190 °C)	(215 °C)
AQM	139.59 (2.04)	17.67 (5.81)	10.76 (1.47)
Rec-ART-AQD (1:1)	121.187 (8.40)	13.36 (6.15)	12.33 (2.29)

To study thermal behaviors of Rec-ART-AQD (1:1), DSC and TGA analysis were used. DSC thermogram of Rec-ART-AQD (1:1) was similar to AQM with one large endotherm followed by two smaller endothermic events at approximate temperatures of 175 °C, 200 °C and 225 °C (Figure 5). Although, the thermal patterns were similar, the energy used was quite different as shown in Table 2. The average endothermic dehydration energy of Rec-ART-AQD (1:1) between 130 °C to 180 °C was shown to be lower than the energy obtained for AQM. Another important aspect to note was that the onsets of the dehydration endotherm began several degrees earlier than AQM. These DSC results suggested that Rec-ART-AQD (1:1) structure was mainly arranged similar to AQM but with minor loosening of the molecular arrangements allowing water molecules to escape at slightly lower temperature than the original AQM.

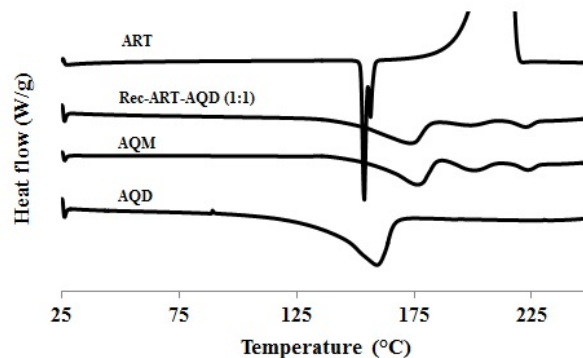


Figure 5 Comparisons of DSC thermograms of starting materials (ART and AQD) and recrystallized crystals: (AQM and Rec-ART-AQD (1:1)) at a heating rate of 10 °C/minute from 25-250 °C.

In addition, the samples were also characterized for their thermal behavior by TGA (Figure 6). ART thermogram displayed weight loss due to degradation starting at 150 °C onwards. Whereas, TGA thermogram of Rec-ART-AQD (1:1) illustrated one step weight loss of 3.1 % by weight starting at 150 °C comparable to monohydrate AQM which showed weight loss of 3.5 % by weight. It could be concluded from these TGA results that the total number of water molecule dehydrated from Rec-ART-AQD (1:1) per gram was slightly less than amount of water molecule released from an equivalent weight of AQM. The results correlate well with the experiments obtained by DSC which may be due to the minor repetitive replacement of some water molecules in the main AQM crystal structure with ART in Rec-ART-AQD (1:1).

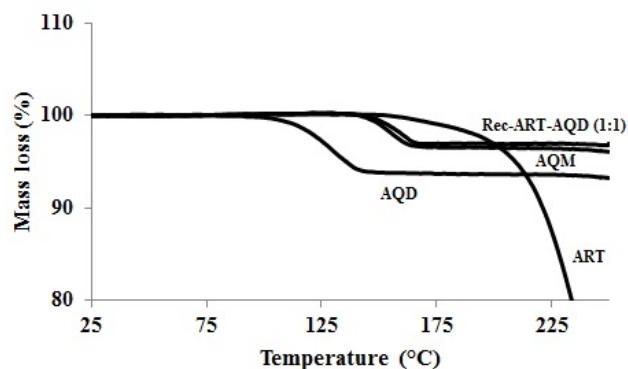


Figure 6 Comparison of TGA thermograms of starting materials (ART and AQD) and recrystallized crystals (AQM and Rec-ART-AQD (1:1)) at a heating rate of 10 °C/minute from 25-250 °C.

The habits of every sample were evaluated by SEM. ART crystals showed needle-like habit as shown in Figure 7 (A). AQD crystals showed pale yellow with small needle-like habit (Figure 7 (B)), whereas AQM was larger rhombohedrons (Figure 7 (C)) with dark orange color.

Rec-ART-AQD (1:1) crystals displayed dark orange color (Figure 7 (D)) similar to AQM. However, when the crystals were observed under high magnification polarized microscope, AQM was transparent while Rec-ART-AQD (1:1) was opaque.

Rec-ART-AQD (1:1) was also evaluated by isothermal dynamic vapor sorption apparatus (DVS) at 30 °C within the relative humidity range of 0-100 %. The result showed that non-significant amount of water was adsorbed on the crystals' surface. The highest amounts of surface moisture collected on ART and Rec-ART-AQD (1:1) crystals equilibrated at 100 %RH (Figure 8) were only 0.21 %w/w and 0.72 %w/w, respectively. While amounts of moisture of AQD and AQM were 1.44 % and 0.44 %, respectively. It could be concluded that every crystal form evaluated in this study were physically stable to wide range of humidity levels and no water uptake in the form of vapor or gas were seen.

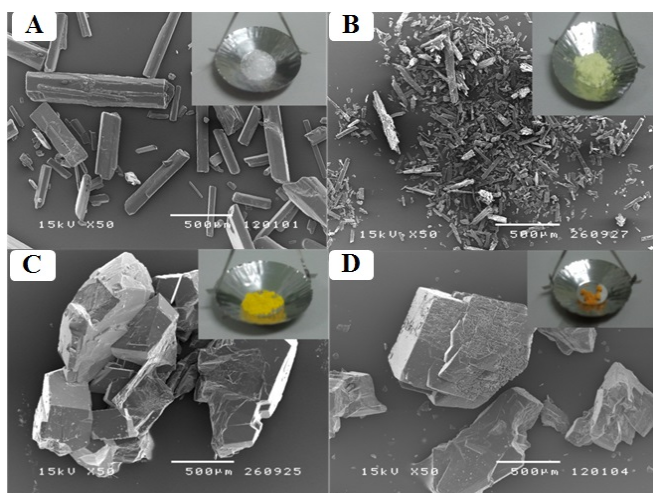


Figure 7 Habits and colors of (A) ART, (B) AQD, (C) AQM and (D) Rec-ART-AQD (1:1) evaluated by SEM (X50).

From the preliminary solid state characterization results, only XRPD technique illustrated a clear distinction between Rec-ART-AQD (1:1) and the control group. In addition, thermal analyses further showed evidences of the incorporation of ART in Rec-ART-AQD (1:1) comparing to control. Therefore, to ensure the incorporation of ART in the crystal lattice, chemical analysis on Rec-ART-AQD (1:1) was done to directly determine the amounts of ART and AQM in the recrystallized structure.

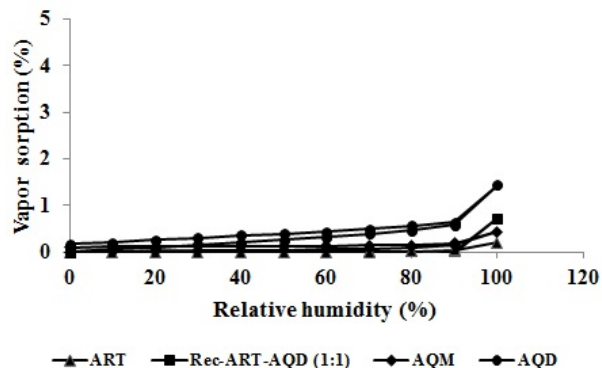


Figure 8 Amounts of water vapor adsorbed on the surfaces of starting materials (ART and AQD) and recrystallized crystals (AQM and Rec-ART-AQD (1:1)) when exposed to various relative humidity at 30 °C.

Table 3 Amounts of ART and AQM in Rec-ART-AQD (1:1) determined by HPLC analysis.

Lot# of Rec-ART-AQD (1:1)	Weight of ART (µg)	Weight of AQM (µg)	Mole ratio (ART:AQM)
1	35.17	964.83*	1:16
2	34.61	965.39*	1:16
3	35.21	964.79*	1:16

*Remark: *Amounts of AQM obtained by subtracting the amounts of analyzed ART from the original weight of Rec-ART-AQD (1:1)*

The amounts of ART and AQM within Rec-ART-AQD (1:1) crystals were evaluated by HPLC. Three different recrystallized batches of Rec-ART-AQD (1:1) were harvested and evaluated. The results showed that the average amount of ART was approximately 35.00 µg in 1000.00 µg of Rec-ART-AQD (1:1) (Table 3). The amount obtained was calculated as mole ratio where it was found to be 1:16 (ART: AQM). From this result, one could explain why some previous solid state characterization techniques could not be used to differentiate between AQM and Rec-ART-AQD (1:1). This is due to the fact that the amount of ART in the crystals was negligibly low, hence, the properties of ART were obscured by the dominant AQM. However, these results confirmed that ART did exist in Rec-ART-AQD (1:1) crystals and distributed within the main crystal structure in a uniform repetitive manner.

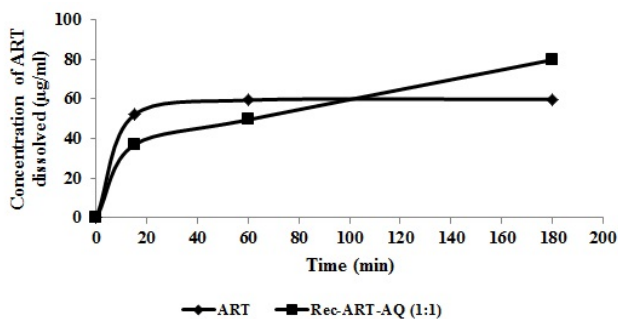


Figure 9 Equilibrium water solubility profiles of ART crystals at 30 °C.

Water solubility of ART was done under controlled temperature at 30 °C. Amount of ART dissolved was initially determined using short intervals to monitor the possible polymorphic transformation that may occur. The result showed that the saturated solubility of ART reached equilibrium at 59.87 µg/mL within 30 minutes (Figure 9). In the case of Rec-ART-AQD (1:1), the normal solubility evaluation could not be used due to two main limitations. First, the amount of Rec-ART-AQD (1:1) crystals produced per batch was very limited and not sufficient to be used in excess. Second, allowing excess Rec-ART-AQD (1:1) crystals to dissolve freely in water to perform solubility experiment, high amount of AQM will dissolve and may interfere with the chemical analysis using HPLC. ART peak in HPLC was undetectable due to very low amount of ART present in Rec-ART-AQD (1:1) crystals and/or the large AQM peak area overlapped with the smaller ART peak. Thus ART peak could not be identified under normal HPLC condition and method.

Therefore, different approach was taken to evaluate the solubility of ART in Rec-ART-AQD (1:1) crystals. Rec-ART-AQD (1:1) crystals were weighed equivalent to two folds of ART saturated solubility (100 µg) by calculating from the ratios obtained in Table 3. The amounts of ART dissolved were determined at various time intervals. The results showed that the amount of ART increased with time upto 180 minutes (Figure 9) where the trend was still continuously increasing. At 180 minutes, the amount of ART dissolved from Rec-ART-AQD (1:1) was found to be 79.81 µg/mL while usual ART saturated solubility was found to be only 59.87 µg/mL. After 15 hours, the amount of ART solubilized out from Rec-ART-AQD (1:1) was found to return to normal saturated solubility of approximately 53.37 µg/mL. This may be due to the recrystallization of ART back to its original solid state structure during the final phase of solubility evaluation. This increased ART solubility in Rec-ART-AQD (1:1) of up to 33.41 % in 180 minutes maybe due to the loosening of the solid state structure detected by DSC and TGA and the possible uniform molecular intervention of ART within Rec-ART-AQD (1:1) crystal lattice as seen by FT-IR.

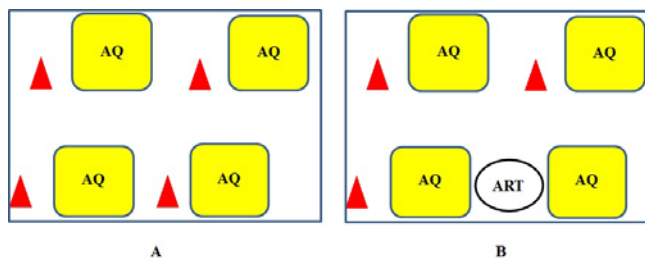


Figure 10 Schematic representations on the possible arrangements of AQ (□), ART (O) and water (Δ) in (A) AQM and (B) Rec-ART-AQD (1:1) crystal lattices.

To confirm the antimalarial activity, all samples were tested against *P. falciparum*, K1 strain. The results showed that IC_{50} of ART (RM) was 0.0030 µg/mL (Table 4). While, IC_{50} of AQD and AQM were essentially the same at 0.0287 and 0.0283 µg/mL, respectively. When Rec-ART-AQD (1:1) was evaluated, the results were not as active as pure ART. However, Rec-ART-AQD (1:1) was found to be slightly more active than AQD and AQM with average IC_{50} of 0.0268 µg/mL. This slight increase in Rec-ART-AQD 1:1 antimalarial activity may be due to the incorporation of the minute amount of ART molecules within the crystal lattice as predicted earlier.

Table 4 Anti-malarial test against *P. falciparum*, K1 strain.

Sample	IC_{50} (µg/mL)	Activity
ART (RM)	0.0030	Active
AQD	0.0287	Active
AQM	0.0283	Active
Rec-ART-AQD (1:1)	0.0268	Active

Hence, many solid state characterization methods were not sufficiently sensitive to detect these minor differences in the incorporation of only a molecule of ART within 16 molecules of AQ in the AQM crystal lattice, such as FT-Raman or ATR-IR. From the results obtained by XRPD and FT-IR, it could be concluded that Rec-ART-AQD (1:1) crystals was a new solid state morphology when comparing to different control group. Thermal analyses by DSC and TGA illustrated minor differences in energy consumption between Rec-ART-AQD (1:1) and AQM. In addition, analyses by HPLC confirmed that ART actually existed in Rec-ART-AQD (1:1) crystal with mole ratio between ART and AQM of 1:16. It can be simplified as an illustration seen in Figure 10 comparing AQM and Rec-ART-AQD (1:1) crystal arrangements. In AQM crystal structure, four molecules of AQ are aligned with four molecules of water. When ART and AQD were cocrystallized by temperature-change technique with ethanol as solvent, the recrystallized crystal incorporated one molecule of ART in, what otherwise, AQM crystal packing.

Conclusion

The cocrystallized crystals of ART and AQD obtained from ethanol at a mole ratio of 1:1 (Rec-ART-AQ (1:1)) showed distinctively different XRPD, FT-IR, DSC and TGA results from control. Amount of ART in Rec-ART-AQ (1:1) was found to be 1 in 16 parts of AQ on mole basis. Despite minor amount of ART in the Rec-ART-AQ (1:1) cocrystals, its equilibrium solubility was shown to be 33.41% higher than ART equilibrium solubility. Rec-ART-AQ (1:1) also showed slight increase in antimalarial activity when compare to AQD. Hence, it could be concluded that Rec-ART-AQD (1:1) was a new solid state morphology with solid state characteristics distinctively different from control and starting materials.

Acknowledgments

Authors would like to acknowledge the Chulalongkorn University Centenary Academic Development Project, Pharmaceutical Research Instrument Center, the Faculty of Pharmaceutical Sciences, Chulalongkorn University and the Faculty of Pharmacy, Siam University for analytical instrument support.

References

- [1] V. Trask. An overview of pharmaceutical cocrystals as intellectual property. *Mol. Pharm.* 4: 301-309 (2007).
- [2] N. Blagden, M. de Matas, P. T. Gavan and P. York. Crystal engineering of active pharmaceutical ingredients to improve solubility and dissolution rates. *Adv. Drug. Deliv Rev.* 59: 617-630 (2007).
- [3] B. Rodríguez-Spong, C. P. Price, A. Jayasankar, A. J. Matzger and N. R. Rodríguez-Hornedo. General principles of pharmaceutical solid polymorphism: A supramolecular perspective. *Advan. Drug Deliv. Rev.* 56: 241-274 (2004).
- [4] D. McNamara, S. Childs, J. Giordano, A. Iarriccio, J. Cassidy, M. Shet, R. Mannion, E. O'Donnell and A. Park. Use of a glutaric acid cocrystal to improve oral bioavailability of a low solubility API. *Pharm. Res.* 23: 1888-1897 (2006).
- [5] P. Vishweshwar, J. A. McMahon, J. A. Bis and M. J. Zaworotko. Pharmaceutical co-crystals. *J.Pharm.Sci.* 95: 499-516(2006).
- [6] S. L. Childs, G. P. Stahly and A. Park. The salt-cocrystal continuum: The influence of crystal structure on ionization state. *Mol. Pharm.* 4: 323-338 (2007).
- [7] A. V. Trask, W. D. S. Motherwell and W. Jones. Physical stability enhancement of theophylline via cocrystallization. *Int. J. Pharm.* 320(1-2): 114-123 (2006).
- [8] R. A. Chiarella, R. J. Davey and M. L. Peterson. Making co-crystals the utility of ternary phase diagrams. *Cryst. Growth. Des.* 7: 1223-1226 (2007).
- [9] G. P. Stahly. Diversity in single- and multiple-component crystals. The search for and prevalence of polymorphs and cocrystals. *Cryst. Growth. Des.* 7: 1007-1026 (2007).
- [10] C. J. Woodrow, R. K. Haynes and S. Krishna. Artemisinins. *Postgrad. Med. J.* 1: 71-78 (2005).
- [11] N. Sittichai. Antimalarial drugs: A current situation. *Thai J. Pharm Sci.* 23: 95-110 (2004).
- [12] K.-L Chan, K.-H. Yuen, H. Takayanagi, S. Janadasa and K.-K. Peh. Polymorphism of artemisinin from *Artemisia annua*. *Phytochemistry.* 46: 1209-1214 (1997).
- [13] E. Ashley, R. McGready, S. Proux and F. Nosten. Malaria. *Travel. Med. Infect. Dis.* 4: 159-173 (2006).
- [14] B. Greenwood. Progress in malaria control in endemic areas. *Travel. Med. Infect. Dis.* 6: 173-176 (2008).
- [15] J. F. Remenar, M. L. Peterson, P. W. Stephens, Z. Zhang, Y. Zimenkov and M. B. Hickey. Celecoxib:Nicotinamide dissociation: using excipients to capture the cocrystal's potential. *Mol. Pharm.* 4: 386-400 (2007).
- [16] S. G. Fleischman, S. S. Kuduva, J. A. McMahon, B. Moulton, R. D. Bailey Walsh, N. Rodríguez-Hornedo and M. J. Zaworotko. Crystal engineering of the composition of pharmaceutical phases: multiple-component crystalline solids involving carbamazepine. *Cryst. Growth. Des.* 3: 909-919 (2003).
- [17] C. B. Davis, R. Bambal, G. S. Moorthy, E. Hugger, H. Xiang, B. K. Park, A. E. Shone, P. M. O'Neill and S. A. Ward. Comparative preclinical drug metabolism and pharmacokinetic evaluation of novel 4-aminoquinoline anti-malarials. *J. Pharm. Sci.* 98: 362-377 (2009).
- [18] G. O. Adjei, W. Kudzi, A. Doodoo and J. A. L. Kurtzhals. Artesunate plus amodiaquine combination therapy: reviewing the evidence. *Drug. Develop. Res.* 71: 33-43 (2010).